Pergamon

Journal of Structural Geology, Vol. 18, No. 12, pp. 1389 to 1397, 1996

0191-8141/96 $15.00+0.00

PII: S0191-8141(96)00060-0

Growth of vertically segmented normal faults

CONRAD CHILDS, ANDREW NICOL,* JOHN J. WALSH and JUAN WATTERSON

Fault Analysis Group, Department of Earth Sciences, University of Liverpool, Liverpool, L69 3BX, U.K.

(*Received* 30 *November* 1995; *accepted in revised form* 15 *July* 1996)

Abstract—The geometry and evolution of vertically segmented normal faults, with dip separations of < *ca* 11.5 m have been studied in a coastal outcrop of finely bedded Cretaceous chalk at Flamborough Head, U.K. Fault trace segments are separated by both contractional and extensional offsets which have step, overlap or bend geometries. The location of fault trace offsets is strongly controlled by lithology occurring at either thin (*ca* 1 mm–8 cm) and mechanically weak marl layers or partings between chalk units. Fault segmentation occurred during either fault nucleation within, or propagation through, the strongly anisotropic lithological sequence. An inverse relationship between fault displacement and number of offsets per length of fault trace reflects the progressive destruction of offsets during fault growth. The preservation of fault offsets is therefore dependent on offset width and fault displacement. Fault rock, comprising gouge and chalk breccia, may vary in thickness by 1.5–2.0 orders of magnitude on individual fault traces. Strongly heterogeneous fault rock distributions are most common on small faults (< 10 cm displacement) and are produced mainly by destruction of fault offsets. Shearing of fault rock with increasing displacement gives rise to a more homogeneous fault rock distribution on large faults at the outcrop scale. Copyright © 1996 Elsevier Science Ltd

INTRODUCTION

Fault segmentation occurs on a wide range of scales (Stewart & Hancock 1991, Peacock & Sanderson 1994a) and in a variety of tectonic settings (Aydin & Nur 1985, Morley *et al.* 1990). Fault segments are transient features and, as faults evolve, segments may coalesce and new segments may form (Segall & Pollard 1980, Wesnousky 1988, Cartwright *et al.* 1995, Childs *et al.* 1995). Coalescence of fault segments results in straightening of the active fault trace and a corresponding change in fault zone architecture. Fault segmentation should therefore be incorporated into models of fault zone growth (Childs *et al.* 1996). Segmented faults can be defined as either vertically or laterally segmented, depending on whether they are identified in cross-section or in map view respectively; vertical and lateral segmentation are end members of the general case of oblique segmentation. Segmentation of normal faults is most commonly described for faults which are segmented in map view (Morley *et al.* 1990, Walsh & Watterson 1990, Peacock 1991, Peacock & Sanderson 1991,1994a, Cartwright *et al.* 1995). Published descriptions of normal fault segmentation in cross-section are rare due to the difficulty of obtaining cross-sectional data of sufficient vertical extent. Here we examine segmented normal faults exposed in a near-vertical cliff section at Danes Dyke on the south coast of Flamborough Head, Yorkshire (see Peacock & Sanderson 1994b, fig. 1c, for location). Due to the anisotropic nature of the finely bedded (ca 0.002–1.5 m) Cretaceous chalk sequence at this locality, the faults are vertically segmented over a range of fault sizes and provide a basis for systematic analysis of the segmentation. The generation and distribution of fault rocks in a fault zone are controlled by a number of factors including fault displacement, rock type, deformation mechanism (Hull 1988), internal fault structure (Blenkinsop 1989) and physical environment (Sibson 1986). Interplay between these and other factors produces highly irregular and complex fault rock thicknesses and distributions. Other than the observation that fault zone thickness increases with net fault displacement (Otsuki 1978, Robertson 1982, 1983, Wallace 1986, Hull 1988, Knott 1994) general rules describing fault rock distribution have not yet been formulated. Segmented faults at Danes Dyke provide an opportunity to isolate the effects of initial fault surface geometry on fault rock distribution. The purpose of this paper is threefold. Firstly, we describe the locations (with respect to bedding), geometries and displacements of segmented faults and present a model for their initiation and evolution. Secondly, we discuss the relationship between initial fault geometry and the distribution of fault rock as developed during subsequent fault growth. Finally, these data are used to develop a model for the evolution of a continuous normal fault trace from a vertically segmented fault trace.

DATA

Many small faults (dip separations 1 mm–11.5 m) are exposed within the Upper Cretaceous, Flamborough Chalk Formation. The sequence consists of interbedded chalks (2 mm–1.5 m thick) and thin (1–80 mm) clay-rich marl units exposed in the 10–20 m high cliff section. Whitham (1993) and Mitchell (1994) provide detailed lithological logs of the sequence which is believed to have attained a maximum burial depth of ca 0.8–1.5 km (Hillis 1995, Stewart & Bailey 1996). Normal, oblique-slip and strike-slip faults are present, but slickenside lineations and bedding displacements indicate that about 75% of

*Present address: Institute of Geological and Nuclear Sciences, PO Box 30368, Lower Hutt, New Zealand.

the faults are normal dip-slip, i.e. with lineations pitching >80° (Peacock & Sanderson 1994b). This study concentrates on these normal faults which have a range of strike directions and dip at 30–90° (average 64°) (Peacock & Sanderson 1992, 1994b). Peacock & Sanderson (1993, 1994b) estimate that these faults accommodate horizontal extensions of *ca* 1% in all directions. It is unclear whether the faults at this locality are of tectonic or glacial origin; contortion and reverse faulting of the chalk immediately adjacent to Danes Dyke shows that glacial deformation has occurred. The processes described here are, however, independent of the origin of the forces which generated the faults.

Data are presented for 73 normal faults with outcrop trace lengths >3 m. Where possible the following variables were measured for the exposed fault trace lengths: orientation, total trace length, number of fault trace segments, trace segment lengths, normal displacement or dip separation on each segment (see Fig. 1), type of trace offset (Fig. 1), trace offset separation (Fig. 1) and length, fault rock thickness (minimum, maximum and average) and maximum fault zone thickness (see below for definition).

FAULT SEGMENTATION AND OFFSET GEOMETRIES

Fault traces at Danes Dyke are generally composed of a series of straight, sub-parallel, non-colinear segments,

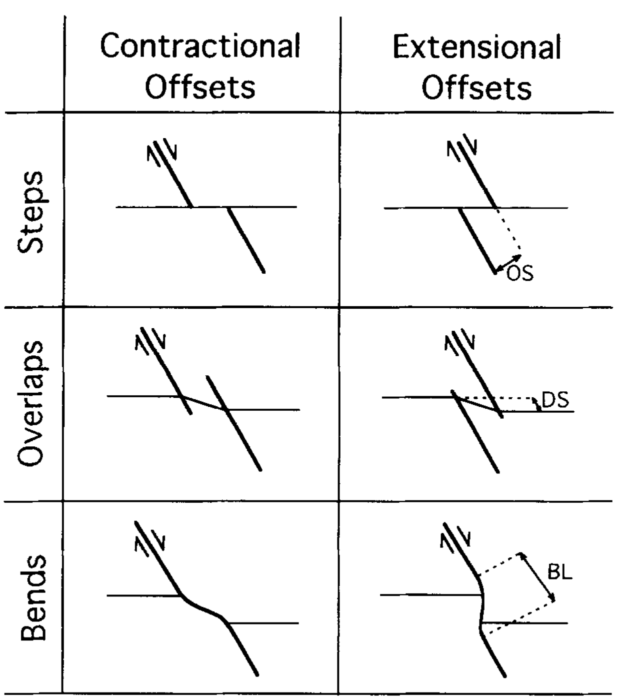

Fig. 1. Schematic diagram showing the six types of fault trace offset geometries encountered at Danes Dyke. The light horizontal line in each figure represents a marl layer or a pronounced parting between chalk units. Fault traces are shown with a heavy line. Fault displacements are shown as increasing with progression from steps to bends. Use of the terms offset separation (OS), dip separation (DS) and bend length (BL) is illustrated.

referred to here as *fault trace segments*. Fault traces at the junctions between adjacent segments may be either discontinuous, as at fault trace steps and overlaps, or continuous, as at fault trace bends (Fig. 1). Junctions between fault trace segments are here termed *fault trace offsets* (or simply offsets), whether or not the fault trace is continuous (Fig. 1). Contractional steps and bends are more common than contractional overlaps, while extensional steps and overlaps are more common than extensional bends. Peacock & Zhang (1994) present a detailed study of selected offsets from Flamborough Head.

The geometries of fault traces and the locations of fault trace offsets are strongly controlled by lithology. The sequence at Danes Dyke consists of three mechanically distinct elements; (a) thick (0.4–1.5 m) chalk units, (b) thin (≤8 cm) marl units and well-defined chalk bedding planes and, (c) finely interbedded chalks and marls forming intervals up to 2 m thick. The effects on fault geometry of the mechanical contrasts are most easily seen for small faults (throws <10 cm) which typically comprise a series of fault trace segments (average dip *ca* 52°) within the chalk layers which are offset across marl units or pronounced bedding planes (Figs. 2a and 3). Fault trace segments within finely interbedded chalk and marl units have shallower dips than those within chalk units. Bedding surfaces separating chalk units and interbedded chalk and marl units are sites of fault refraction of up to 30°. Faults with displacements of <*ca.* 1 cm in finely interbedded chalk and marl units commonly have a well defined staircase trajectory. The extent to which lithology controls the locations of fault trace offsets is illustrated by the two faults shown in Fig. 3, which each have offsets at the same horizons. In three dimensions, offsets are therefore aligned parallel to bedding and approximately normal to the fault slip direction.

Individual fault traces may have a consistent sense of offset; either all contractional (Fig. 2a) or all extensional offsets (Fig. 3), or a mixed offset sense. Faults with all contractional offsets generally have low overall, or gross, dips (*ca.* 30–45°) (Fig. 2a), while structures with all extensional offsets tend to have high overall dips (70–80°) (Fig. 3). This relationship arises because dips of individual segments within a particular mechanical unit tend to be similar.

Fault trace offsets are foci of high strain and high displacement gradients (Peacock & Sanderson 1991, Childs *et al.* 1995). At Danes Dyke the fault trace offsets accommodate dip-parallel displacement gradients at fault trace segment tip regions (0.05–1.32, mean = 0.65) which are 1–2 orders of magnitude higher than the gradient (0.013–0.05) elsewhere on the fault traces (Fig. 4). For faults with displacements >*ca.* 5 cm, high strains at offsets are accommodated by flow within clay-rich units, folding of finely bedded units and by fracturing and brecciation (see fig. 3 of Peacock & Zhang 1994). At contractional offsets, radial fracturing of hangingwall and/or footwall chalk units is common (Fig. 2b) and 100% thinning of clay units may occur (Fig. 2a, arrowed offset). Flow within clay units at extensional offsets can

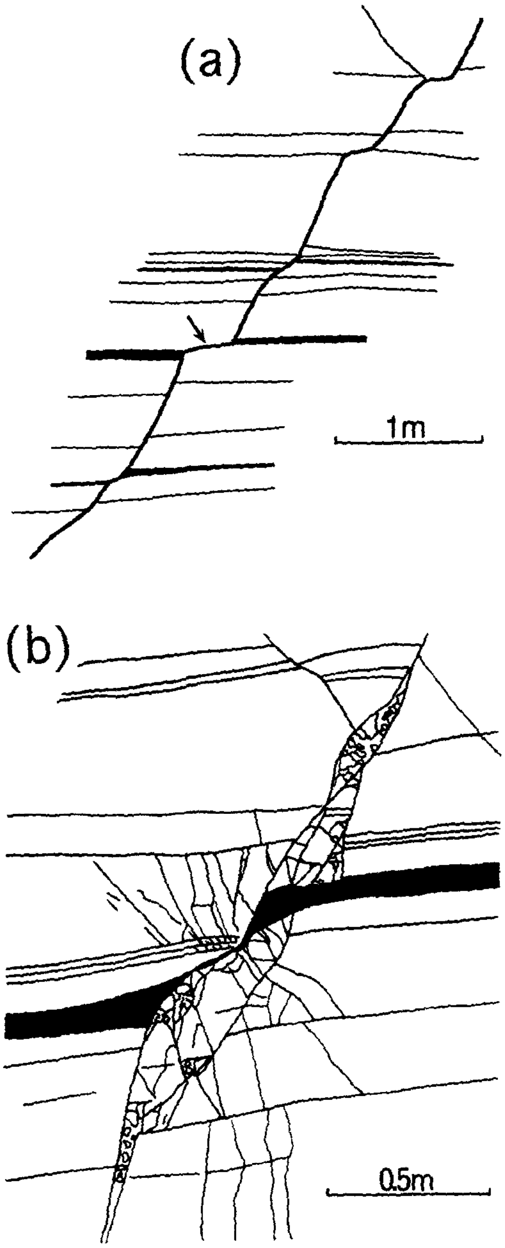

Fig. 2. Examples of contractional offsets exposed in a near-vertical chalk cliff at Danes Dyke. (a) Fault trace, continuous heavy line, with only contractional offsets. The fault bend arrowed is discussed in the text. (b) Contractional bend with radial fracturing and fault bounded lenses of fractured/brecciated chalk. Marl units are shown in black, intervening chalk units are un-ornamented and light sub-horizontal lines indicate pronounced bedding planes.

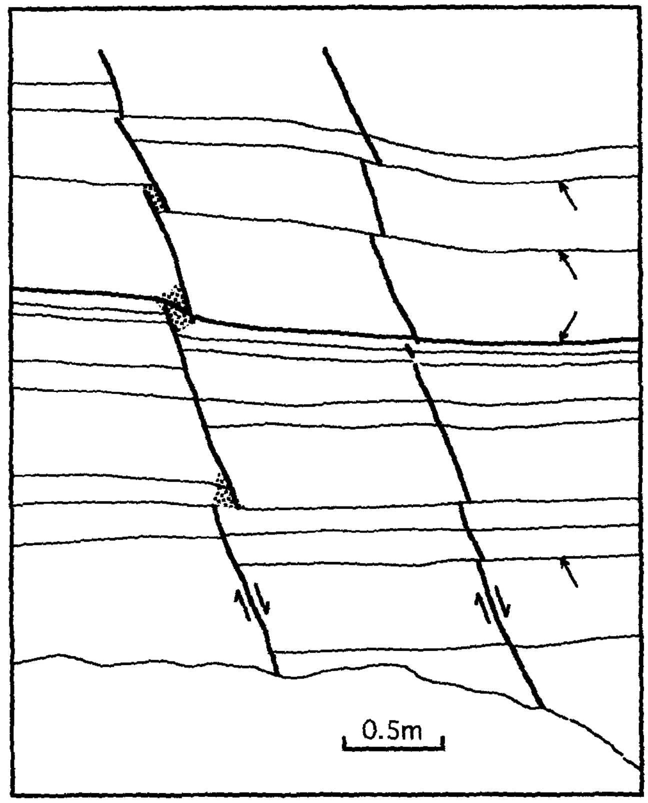

Fig. 3. Two fault traces with only extensional offsets, exposed in a near-vertical cliff at Danes Dyke. Offsets occur at the same bedding planes on each fault. The fault on the left has an average displacement of 15 cm and that on the right, displacements of 1–2 cm. Stippled areas indicate intensely deformed or brecciated chalk. Sub-horizontal lines indicate thin marl units (arrowed) and pronounced bedding planes. The overall dip of both faults is *ca.* 75°.

give rise to clay thicknesses within the offset which are several times those of the source clay units. At displacements > 50 cm, zones of intense fracturing and localised pods of fault rock associated with straight or gently curved fault traces are characteristic and are attributed to the complete destruction of pre-existing fault trace offsets.

Steps are the most common type of fault trace offset at low displacements (< 5 cm) while bends and overlaps are more common for higher displacements (> 10 cm). Peacock & Zhang (1994) noted that displacements are generally lower at contractional steps than at contractional bends. These observations suggest that most offsets originate as steps which are replaced at higher displacements by overlaps or bends. This evolution of structure is illustrated by comparison between the contractional step arrowed in Fig. 2(a) and the contractional bend in Fig. 2(b). High displacement gradients at the step (Fig. 2a) are accommodated by thinning of the marl unit. Increase in the displacement on this fault would cause failure of the step. The step would initially fail by fracturing of the chalk with the fractures radially centred on the step; this radial fracturing is clearly seen in the hangingwall of the bend in Fig. 2(b). Further increase in displacement would lead to progressive fracture and brecciation of the chalk at the site of the original step. The footwall of the bend in Fig. 2(b) demonstrates radial fracturing which has been superseded by a through-going slip surface. A similar evolution of structure for extensional steps is illustrated by the two fault traces shown in Fig. 3. Extensional steps across thin marl units and pronounced chalk bedding discontinuities on the low displacement fault coincide, in terms of position within the lithological sequence, with sites of intense deformation and brecciation on the larger displacement fault. Offset of fault trace segments is still preserved on the large displacement fault but would not be apparent were the displacement to become larger than ca 50 cm. The failure of extensional steps is not accompanied by radial fracturing of adjacent chalk units.

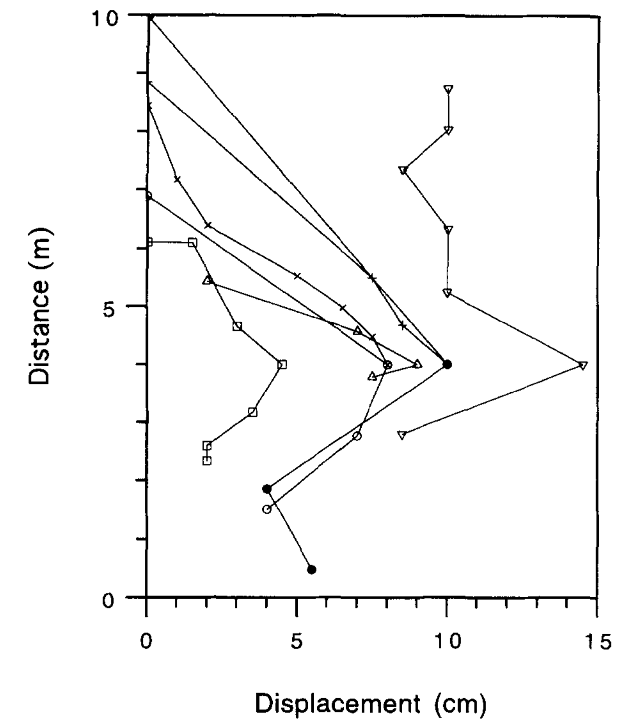

Fig. 4. Displacement profiles along seven segmented fault traces at Danes Dyke. Each data point represents a single fault trace segment and distance is to the centre of each fault trace segment as measured parallel to the fault trace. Displacement values are dip separations of faulted beds. The profiles are located so that their points of maximum displacement coincide. Displacements at fault trace offsets are often significantly lower than those at segment mid-points; high displacement gradients at segment boundaries are accommodated by bed rotation or by thickening and thinning of marl units. Displacements could not be estimated for all segments and data are included only for faults with four or more measurements (i.e. with ≥4 segments).

Four models for the formation of contractional fault bends at Flamborough were discussed by Peacock & Zhang (1994):

(i) An originally planar fault is affected by later compaction or pressure solution.

(ii) An originally planar fault is offset by bedding-parallel shear across marl units.

(iii) A propagating fault is refracted as it passes through less competent or more competent units.

(iv) Two initially overstepping faults propagate and link across a marl unit.

These are also the appropriate models to consider when explaining the entire range of fault trace offset geometries observed at Danes Dyke (Fig. 1). We concur with Peacock & Zhang (1994) that models (i) and (ii) are improbable. Model (i) requires tens of centimetres of compaction or pressure solution and while bedding-parallel stylolites are abundant at Danes Dyke, there is no evidence for solution on this scale. Model (ii) requires a common sense of offset across an individual marl unit, which does not occur. Furthermore, neither of these models explains the occurrence of fault trace overlap and model (i) cannot produce extensional offsets.

Fault bends due to refraction (model iii) are common where a fault passes through finely interbedded chalks and marls into more competent chalk layers above and below. In these cases, the dips of fault traces within the finely interbedded units may be 30° shallower than in the over- and under-lying chalk units. Fault trace refraction gives rise to fault trace bends, with separations <50 cm and bend lengths (40–200 cm) proportional to the thickness of the interbedded unit. However, the fault refraction model cannot account for large separation fault trace offsets across either individual thin (≤8 cm) marl units or pronounced chalk bedding discontinuities, where the fault trace within the marl unit is parallel to bedding, or nearly so. Finally, extensional fault trace offsets across either incompetent units or pronounced bedding planes cannot be due to refraction, as this would require fault traces to steepen (generally through the vertical) within incompetent units.

Model (iv) is the mechanism which best accounts for the fault trace offset geometries observed at Danes Dyke and, in particular, is the only model consistent with the occurrence of fault trace overlaps. We conclude that, apart from those relatively large bends caused by refraction, offsets result from overlaps/linkages between fault trace segments which were, initially, isolated in cross-section. The development of contractional steps and bends by this mechanism is similar to that proposed for thrust propagation by Eisenstadt & De Paor (1987) whereby isolated ramps are subsequently linked by bedding parallel flats. A similar model for normal faults was proposed by Peacock & Sanderson (1992).

Although individual fault trace segments are isolated in 2-D or 3-D, i.e. the fault trace is not continuous between adjacent offset segments, their relative locations are not random but ordered (Figs. 2a and 3). Using the densities of faults which both dip towards NE (the more numerous faults) and transect individual thick (>0.5 m) chalk units, we have estimated the probable number of segments, in three or more adjacent chalk layers but otherwise randomly located, which would by chance be aligned to form a single fault trace, i.e. offset separation <0.5 m. The number of such fault traces is 1 order of magnitude less than the number of fault traces comprising 3 or more segments which are actually present. Fault traces consisting of up to 14 individual sub-parallel fault trace segments are most unlikely to have resulted from linkage of randomly located structures. The non-random spatial distribution of the initially separate fault trace segments points to an underlying control of their locations. Segmented fault traces are kinematically single structures with aggregate displacement patterns similar to those of non-segmented faults (Barnett *et al.* 1987, Walsh & Watterson 1988,1989, Peacock & Sanderson 1991, Dawers & Anders 1995) even when their displacements are small (<5 cm; Fig. 4), indicating a systematic relationship between the individual fault trace segments. Although co-location of some segments may occur by chance, we suggest that segmented fault traces are organised structures which form at an early stage of fault nucleation and propagation.

A segmented fault trace represents either a section through the centre of a small fault or a section close to the tip-line of a large fault on which there is higher displacement out of the plane of section. In the latter case the location of the fault trace, with segments aligned but isolated in 2-D, would be either within the tip-line of the parent fault or in a process zone beyond the tip-line. In 3-D, the apparently separate fault trace segments are likely to be connected to one another and to the parent fault surface, only if the section is within the tip-line of the parent fault. In the alternative case, in which the observed cross-section is the nucleus of a small fault, the fault segments are likely to be separate in both two and three dimensions. In both this case and when the fault trace is distal from the tip-line of a larger fault, the individual fault trace segments occur within a narrow planar yield zone defined, prior to yielding, by relatively high elastic shear strains. In this model, failure occurs independently within each chalk unit but is confined within the planar nucleation process zone.

Both the propagation and the nucleation segmentation processes can be conceptualised in terms of an elastic monocline or proto-shear zone preceding and localising

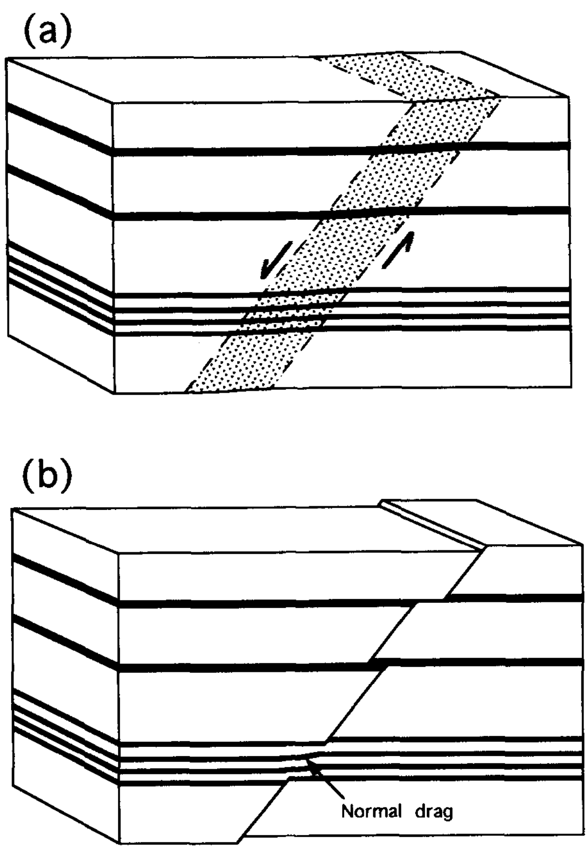

Fig. 5. Schematic diagram illustrating the development of a vertically segmented normal fault in an interbedded chalk and marl (heavy black lines) sequence. Failure within the proto-shear zone, or monocline (stippled in a), results in the vertically segmented fault trace shown in (b). The rock volume represented in (a) may be either beyond the tip-line of a propagating fault surface (propagation process, see text) or in unfaulted rock (nucleation process). The equivalent faulted rock volume shown in (b) occurs either distally with respect to the propagating fault tip-line, or, in the case of the nucleation model, remotely from pre-existing faults. The discrete, or discontinuous, displacement characteristic of the chalk units in (b) is expressed in finely interbedded chalks and marls by ductile normal drag, or continuous displacement. For simplicity, the proto-shear zone in (a), although shown as parallel sided, may vary in thickness between units of different rheology.

the formation of a segmented fault trace (Fig. 5a). Fault trace segments are confined to the proto-shear zone the thickness of which is at least equal to the largest fault trace offset separation (Fig. 5b). Under non-brittle conditions the concentration of elastic shear strain would result in a permanent strain in the form of a ductile shear zone, as in those parts of the sequence with a high marl content where some fault displacement is accommodated by ductile shear, or normal drag (Fig. 5b).

The formation of pre-failure micro-scale process zones is observed in experimental deformation of sandstones and granites (Lockner *et al.* 1992, Reches & Lockner 1994) although they are > 2 orders of magnitude smaller than the segmented faults at Danes Dyke.

Pre-failure localisation of small shear strains and dilatant volumetric strains is also observed in dense sand (Roscoe 1970). The zone in which pre-failure strains occur in sands is analogous to the proto-shear zone proposed here. In the experiments reported by Roscoe (1970), shear strains up to 0.1 were observed prior to failure. In stronger materials we would expect failure to occur at much smaller elastic strains.

FAULT TRACE OFFSET SYSTEMATICS

Figure 6 illustrates the relationship between fault displacement and fault trace offset separation (Fig. 1) for separations of 2–70 cm (average 10 cm) on fault traces with displacements of 1–500 cm. Contractional and extensional offset data are separately identified but show similar distributions. Figure 6 shows that small offset separations (< 5 cm) of traces occur mainly on faults with small displacements (1–10 cm), while larger separations (> 15 cm) occur on faults of all sizes (1–

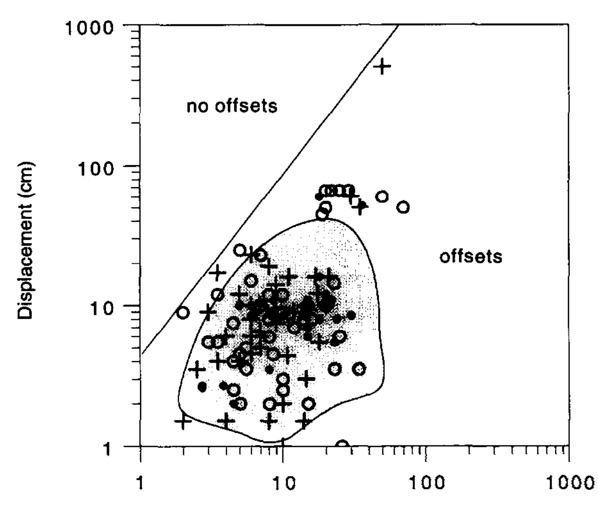

Fig. 6. Log–log plot of displacement vs fault trace offset separation for extensional offsets (crosses, $N = 42$), contractional offsets with radial fractures (filled circles, $N = 26$) and without radial fractures (open circles, $N = 47$). Contractional offsets ($N = 102$) from Peacock & Zhang (1994) plot in the shaded region. The straight line separates fields in which offsets do and do not occur and indicates the minimum offset separation for a given displacement.

500 cm). This difference reflects an increase in minimum separation with increasing displacement, due to progressive destruction of fault trace offsets during fault growth and increase in displacement. The upper boundary to the data in Fig. 6 defines the minimum offset separation of traces for a given displacement. For separations of 1–10 cm, the upper limit of displacement is between 5 and 8 times the separation. The absence of data on the right-hand side of the plot (Fig. 6) is due to (a) the ambiguity which inevitably arises when the offset separation is much larger than the fault displacement, and (b) the difficulty in identifying larger separations due to the restricted height of the outcrop.

The data presented in Fig. 6 are interpreted in terms of a growth sequence. When a fault trace is formed, whether as a tip-line or as a nucleation process zone, it contains numerous offsets with a range of separations, the loci of which would be represented on Fig. 6 as a sub-horizontal line approximately coincident with the x-axis. As the displacement on the fault increases, individual offsets become sites of intense deformation which eventually results in them being breached and destroyed. Obliteration of trace offsets occurs first on those structures with smallest separations with progressively larger separation offsets being breached and destroyed at higher displacements. The locus of offset separation values for a fault trace of given displacement is therefore defined by a horizontal line terminating at the line separating the fields in which offsets do and do not occur.

While preservation of fault trace offsets is mainly a function of the ratio between offset separation and the fault displacement, preservation is also dependent on the mechanical properties of units at, or adjacent to, the offset. For example, steps located on a 7–8 cm thick marl unit have an enhanced life expectancy because high strains can be accommodated by plastic flow. Conversely, contractional bends with radial fractures appear to have a reduced life expectancy, as intense fracturing enables an offset to be breached more readily than would otherwise be the case; this effect is indicated by the relatively low maximum displacement accommodated by these offsets (Fig. 6).

The progressive destruction of fault trace offsets with increasing fault displacement is also reflected in the number of preserved offsets per unit fault trace length for a given displacement (Fig. 7). The spread of data in Fig. 7 partly reflects the influence of the lithological sequence on the formation and development of offsets. For example, the number of fault trace offsets per unit length of fault trace in finely bedded rocks (bed thicknesses 5–10 cm) tends to be higher than where the beds are thicker (0.4–1.5 m). However, offsets in finely bedded units are also likely to have smaller separations and to be more readily breached. Therefore, segmented faults in a finely bedded sequence would evolve along a relatively steep line running diagonally across the data field in Fig. 7. Destruction of offsets with increasing displacement causes faults to become less segmented and therefore progressively straighter as they grow. Wesnousky (1988) reached similar conclusions for segmented strike-slip faults. These conclusions are valid for situations in which the fault offset axis (i.e. the upper or lower tip-lines of fault segments or the hinge line of a fault bend or step) is at a high angle to the fault slip vector (the displacement-normal offset of Peacock & Sanderson 1991). Fault offsets with axes parallel to the fault slip vector (displacement-parallel offsets) are not expected to behave in the same manner and bends in traces of normal faults seen in map view are not necessarily unstable structures.

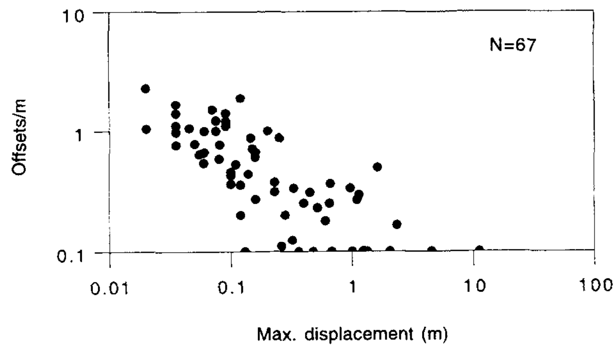

Fig. 7. Log–log plot of offsets per metre of fault trace length vs maximum displacement, for 67 fault traces. Fault traces with no offsets are arbitrarily assigned a value of 0.1 offsets per metre. Offsets per metre decreases with increasing maximum displacement due to offset destruction during fault growth. The accuracy of estimated offsets per metre decreases with increasing maximum displacement as the exposed fault trace length becomes less representative of the total dip length of a fault trace.

FAULT ZONE THICKNESS AND GROWTH

Concentration of deformation around fault offsets has implications for the spatial and temporal variability of fault zone thicknesses. Fault zone and fault rock thicknesses were recorded for 30 fault traces which accommodate dip separations of 0.02–11.5 m and all of which extend for at least 3 m in length. As discussed by Evans (1990), when reporting data on fault zone thicknesses, criteria for distinguishing fault rock and non-fault rock need to be stated. The term 'fault rock' here refers to gouge and breccia only, while the term 'fault zone' includes fault rock together with mildly deformed or intact blocks enclosed by two or more slip-surfaces. In those cases where the fault is represented by a single zone of fault rock, the fault rock and fault zone widths are the same. The distinction between fault rock and non-fault rock is dependent on the scale of observation and although our thickness measurements are internally consistent they are not necessarily directly comparable with other data.

Both fault rock and fault zone thicknesses vary by 1.5–2.0 orders of magnitude along individual fault traces. Estimated mean values of fault rock thicknesses and maximum values of fault zone widths are shown in Fig. 8. The mean fault rock thickness along a fault trace was estimated in the field by averaging between 3 and 5 thickness measurements which were representative of the variation in thickness on the fault trace. To test the

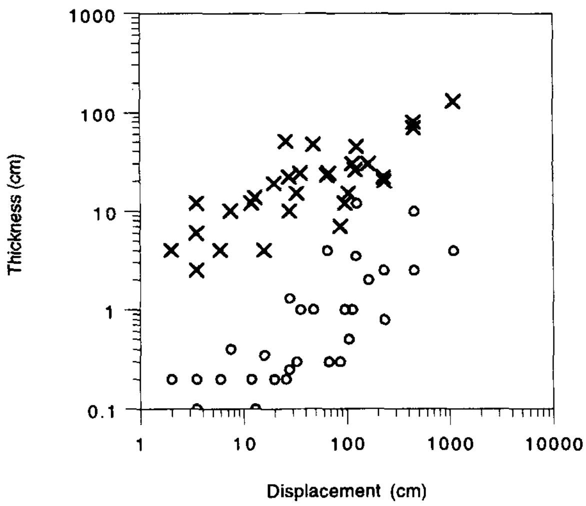

Fig. 8. Log–log plot of maximum fault zone thickness (crosses) and average fault rock thickness (open circles) vs maximum displacement for 30 faults at Danes Dyke. See text for definitions of fault zone and fault rock.

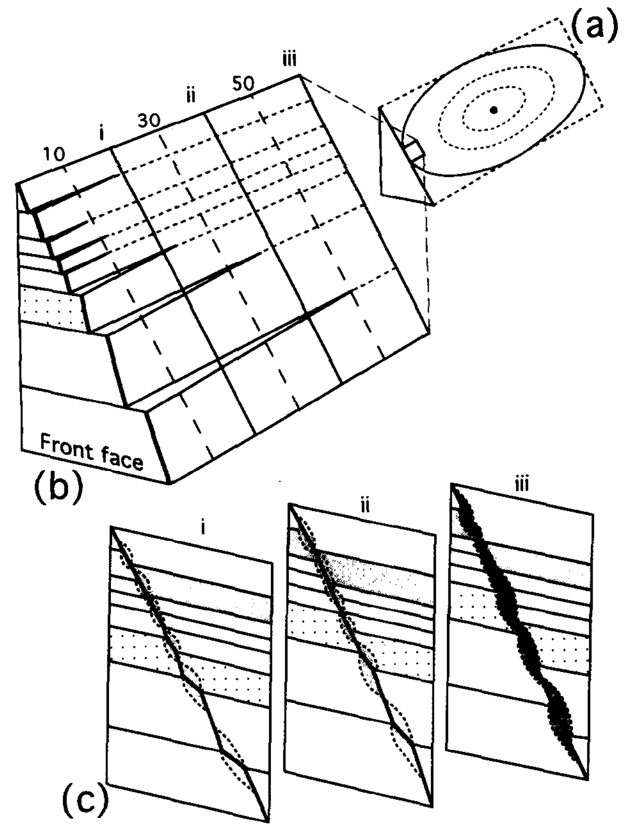

Fig. 9. Schematic block diagrams (a) and (b) and cross-sections (c) illustrating the evolution of a fault with only contractional offsets. (a) An ideal elliptical normal fault surface showing fault displacement contours (broken lines) and tip-line (solid line). (b) Enlargement of the lateral tip region of the fault in (a) showing the detailed geometry of the fault surface. The front face of (b) illustrates the fault cross-sectional geometry in the tip-line region with the discontinuous segmented fault trace shown by heavy lines. Light broken lines show the trace of bedding intersections on the fault surface and steeply pitching heavy broken lines are 10, 30 and 50 cm displacement contours. The locations of cross-sections (i)–(iii) are indicated. (c) Cross-sections (i)–(iii) show progressive straightening of the fault trace and an increase in the area of fault-related deformation (shaded) which indicates fault rock, fault zone and areas of intense fracturing.

accuracy of this procedure, thicknesses were measured every 5 cm along selected fault traces. The thickness data obtained in this way for an individual fault trace yield an asymmetric frequency distribution. Mean thickness values estimated by the simple method lie closer to the modes of these distributions than to the means but the simple estimates of 'mean' fault rock thickness have correct relative values. Fault rock thicknesses for faults with displacements <0.5 cm are not shown in Fig. 8 as they are <1 mm and could not be determined accurately at outcrop. Along small faults (<10 cm displacement), the greatest fault rock thicknesses occur within, or immediately adjacent to, fault trace offsets and smallest thicknesses are on intervening segments. Figure 8 shows that both fault rock and fault zone thicknesses increase as displacement increases. While fault rock thickness appears to scale linearly with displacement, consistent with the results of Hull (1988), fault zone thickness does not. However, since only a small proportion (probably <10%) of the total dip-parallel trace length of larger faults (displacement >50 cm) could be sampled, maximum fault zone thicknesses for these faults are likely to be underestimated. Our observations indicate that offset-related deformation is the primary source of fault rocks on these faults. Other mechanisms by which fault rock thickness increases with increasing displacement appear not to have been significant at Danes Dyke. Evidence for strain hardening of fault zones (Hull 1988) was not observed. Progressive attrition of wall rocks on straight fault segments (Robertson 1982, 1983) was also not evident but may occur on a scale smaller than could be observed in outcrop. The progressive destruction of fault trace offsets which we have described could, when considered on a larger scale, be regarded as an attrition process.

A model for the evolution of a vertically segmented fault trace to a through-going fault zone is shown schematically in Fig. 9. The process is illustrated by four cross-sections through a fault surface (one at the fault tip-line (Fig. 9b, Front face) and three progressively more distant from the tip-line (Fig. 9c, i–iii)), representing the change in fault zone structure with increasing displacement i.e. towards the fault centre. Although we have chosen to illustrate the evolutionary progress by reference to spatial variation of fault zone structure on a single fault, the progression is the same as that at a single point on a fault surface during fault growth.

In the tip region of the fault surface (Fig. 9b) the fault trace comprises a series of straight parallel segments separated by contractional steps at bedding interfaces. The steps are parallel to the fault/bedding intersection and have a range of separations. For displacements of 0–*ca* 0.5 cm, fault rock thicknesses are too small (<1 mm) to measure at outcrop (Fig. 9b, tip-line section). At displacements of 0.5 cm to 10–20 cm, i.e. up to section (i) in Fig. 9(b) the smaller offsets of the fault surface/trace are breached and larger offsets are sites of fracturing and localised brecciation. As a consequence of offset destruction, fault rock and fault zone thicknesses are substantially increased within and around offsets, but remain small (<1 mm) on the intervening fault segments so producing a heterogeneous distribution of fault rock (Fig. 9c, section i). At higher displacements, progressively larger offsets are destroyed (Fig. 6) and the length of fault trace with a measurable (> 1 mm) thickness of fault rock is also increased (Fig. 9c, section ii). The fractured and brecciated products of offset destruction are displaced and distributed over the fault surface, providing a more regular fault rock distribution. All the offsets on the fault surface are destroyed at high displacements (> 70 cm) and the fault trace is approximately straight and everywhere has a measurable (> 1 mm) thickness of fault rock (Fig. 9c, section iii).

DISCUSSION

Because the rheological differences between the chalks and marls exposed at Danes Dyke are pronounced, the geometric irregularities of the faults initiated within and propagated through the sequence are also pronounced (Fig. 2a). In a sequence with a less pronounced mechanical anisotropy, the fault segmentation would probably be more subdued, with smaller and fewer offset separations than at Danes Dyke. The fault geometries observed at Danes Dyke nevertheless provide a basis for observation and interpretation of similar, but more subtle, fault trace geometries in other types of sequence.

Fault segmentation has been observed at Danes Dyke on faults with up to 5 m displacement, this upper limit being simply a function of the vertical extent of the outcrop and, given a larger outcrop, the displacement limit would be extended. Faults with several 10's of metres displacement, or greater, will also be vertically segmented if the faulted sequence is mechanically anisotropic on the appropriate scale.

If vertical segmentation is a common feature of normal faults with 10's of metres displacement then the question arises of why it has only rarely been reported? Few outcrops are of sufficient vertical extent to allow identification of large fault trace offsets. Seismic reflection data, on the other hand, often span a sufficiently large (> 500 m) vertical interval but usually have relatively poor lateral resolution, particularly along and adjacent to faults. While large separation (> 100 m) overlap zones on normal faults have been recognised on seismic cross-sections (Chapman & Meneilly 1991, Nicol *et al.* 1996), offsets with separations < 100 m at depths > *ca* 1 km cannot be resolved in seismic data. The apparent scarcity of vertical segmentation on normal faults is likely, therefore, to be due mainly to data limitations.

Two models for the formation of segmented faults in cross-section have been proposed, i.e. propagation related and nucleation related. Only propagation related processes are likely to occur over a wide scale range and to produce segmentation of faults with throws of 100's of metres.

Vertical offsets are likely sites of intense deformation, in the form of intense fracturing and rapid thickening or thinning of incompetent units close to the fault. Such areas are potential sites for enhanced mineralisation (Newhouse 1942, Park & MacDiarmid 1964, p69, Hagemann *et al.* 1992) or for either increase or decrease of shale smear, with consequent negative or positive effects on fluid flow across or adjacent to a fault.

CONCLUSIONS

(1) Vertical segmentation of normal fault traces is common in the finely bedded sequence of Cretaceous chalk at Flamborough Head, U.K. Fault trace segments are offset across contractional and extensional steps, overlaps and bends.

(2) The location of fault trace offsets is lithologically controlled with offsets occurring preferentially at mechanically weak layers.

(3) Individual fault trace segments either initiate as separate structures which are located in and aligned with a proto-shear zone, within which brittle failure is localised to form a fault, or initiate as structures which are spatially associated with the tip-line region of a propagating fault and which may or may not be connected in 3-D, according to their location relative to the tip-line.

(4) With increasing fault displacement, fault trace offsets are progressively destroyed. The preservation of an offset depends both on the fault displacement and on the offset separation, with progressively larger separation offsets destroyed at progressively higher displacements.

(5) Fault rock at Danes Dyke is generated primarily by the progressive destruction of fault trace offsets.

Acknowledgements—This research was part funded by the OSO/NERC Hydrocarbon Reservoirs LINK Programme (project 827/7053) and by the CEC Joule 2 Reservoir Engineering Project (Contract No. JOU2-CT92-0182). We are grateful to Marie Eeles for drafting the diagrams and to members of the Fault Analysis Group for useful discussions. Atilla Aydin, Richard Lisle and Eugene Robertson are thanked for their helpful reviews. The manuscript also benefited considerably from comments by David Peacock.

REFERENCES

Aydin, A. & Nur, A. 1985. The types and role of stepovers in strike-slip tectonics. In: *Strike-slip Deformation, Basin Formation and Sedimentation* (edited by Biddle, K. T. & Christie-Blick, N.). *Spec. Publ. Soc. Econ. Palaeo. Min.* **37**, 35–44.

Barnett, J. A. M., Mortimer, J., Rippon, J., Walsh, J. J. & Watterson, J. 1987. Displacement geometry in the volume containing a single normal fault. *Bull. Am. Ass. Petrol. Geol.* **71**, 925–937.

Blenkinsop, T. G. 1989. Thickness–displacement relationships for deformation zones: Discussion. *J. Struct. Geol.* **11**, 1051–1054.

Cartwright, J. A., Trudgill, B. & Mansfield, C. S. 1995. Fault growth by segment linkage: an explanation for scatter in maximum displacement and trace length data from the Canyonlands Grabens of S. E. Utah. *J. Struct. Geol.* **17**, 1319–1326.

Chapman, T. J. & Meneilly, A. W. 1991. The displacement patterns associated with a reverse-activated, normal growth fault. In: *The Geometry of Normal Faults* (edited by Roberts, A. M., Yielding, G. & Freeman, B.). *Spec. Publ. geol. Soc. Lond.* **56**, 183–192.

Childs, C., Watterson, J. & Walsh, J. J. 1995. Fault overlap zones within developing normal fault systems. *J. geol. Soc. Lond.* **152**, 535–549.

Childs, C., Watterson, J. & Walsh, J. J. 1996. A model for the structure and development of fault zones. *J. geol. Soc. Lond.* **153**, 337–340.

Dawers, N. H. & Anders, M. H. 1995. Displacement–length scaling and fault linkage. *J. Struct. Geol.* **17**, 607–614.

Eisenstadt, G. & De Paor, D. G. 1987. Alternative model of thrust-fault propagation. *Geology* **15**, 630–633.

Evans, J. P. 1990. Thickness–displacement relationships for fault zones. *J. Struct. Geol.* **12**, 1061–1065.

Hagemann, S. G., Groves, D. I., Ridley, J. R. & Vearncombe, J. R. 1992. The Archean lode gold deposits at Wiluna, Western Australia: High-level brittle-style mineralization in a strike-slip regime. *Econ. Geol.* **87**, 1022–1053.

Hillis, R. R. 1995. Quantification of Tertiary exhumation in the United Kingdom southern North Sea using sonic velocity data. *Bull. Am. Ass. Petrol. Geol.* **79**, 130–152.

Hull, J. 1988. Thickness–displacement relationships for deformation zones. *J. Struct. Geol.* **10**, 431–435.

Knott, S. D. 1994. Fault zone thickness versus displacement in the Permo–Triassic sandstones of NW England. *J. geol. Soc. Lond.* **151**, 17–25.

Lockner, D. A., Byerlee, J. D., Kuksenko, V., Ponomarev, A. & Sidorin, A. 1992. Observations of quasistatic fault growth from acoustic emissions. In: *Fault Mechanics and Transport Properties of Rocks* (edited by Evans, B. & Wong, T.-F.). Academic Press, 3–31.

Mitchell, S. F. 1994. New data on the biostratigraphy of the Flamborough Chalk Formation (Santonian, Upper Cretaceous) between South Landing and Danes Dyke, North Yorkshire. *Proc. Yorks. geol. Soc.* **50**, 113–118.

Morley, C. K., Nelson, R. A., Patton, T. L. & Munn, S. G. 1990. Transfer zones in the East African rift system and their relevance to hydrocarbon exploration in rifts. *Bull. Am. Ass. Petrol. Geol.* **74**, 1234–1253.

Newhouse, W. H. 1942. *Ore Deposits as Related to Structural Features.* Princetown University Press.

Nicol, A., Watterson, J., Walsh, J. J. & Childs, C. 1996. The shapes, major axis orientations and displacement patterns of fault surfaces. *J. Struct. Geol.* **18**, 235–248.

Otsuki, K. 1978. On the relationship between the width of shear zone and the displacement along fault. *J. geol. Soc. Jap.* **84**, 661–669.

Park, C. F. & MacDiarmid, R. A. 1964. *Ore Deposits.* Freeman, San Francisco.

Peacock, D. C. P. 1991. Displacements and segment linkage in strike-slip fault zones. *J. Struct. Geol.* **13**, 1025–1075.

Peacock, D. C. P. & Sanderson, D. J. 1991. Displacements, segment linkage and relay ramps in normal fault zones. *J. Struct. Geol.* **13**, 721–733.

Peacock, D. C. P. & Sanderson, D. J. 1992. Effects of layering and anisotropy on fault geometry. *J. geol. Soc. Lond.* **149**, 793–802.

Peacock, D. C. P. & Sanderson, D. J. 1993. Estimating strain from fault slip using a line sample. *J. Struct. Geol.* **15**, 1513–1516.

Peacock, D. C. P. & Sanderson, D. J. 1994a. Geometry and development of relay ramps in normal fault systems. *Bull. Am. Ass. Petrol. Geol.* **78**, 147–165.

Peacock, D. C. P. & Sanderson, D. J. 1994b. Strain and scaling of faults in the chalk at Flamborough Head, U.K. *J. Struct. Geol.* **16**, 97–107.

Peacock, D. C. P. & Zhang, X. 1994. Field examples and numerical modelling of oversteps and bends along normal faults in cross-section. *Tectonophysics* **234**, 147–167.

Reches, Z. & Lockner, D. A. 1994. Nucleation and growth of faults in brittle rocks. *J. geophys. Res.* **99**, 159–173.

Robertson, E. G. 1982. Continuous formation of gouge and breccia during fault displacement. In: *Issues in Rock Mechanics* (edited by Goodman, R. E. & Heuze, F. E.). AIMME, New York, 397–404.

Robertson, E. G. 1983. Relationship of fault displacement to gouge and breccia thickness. *Am. Inst. Min. Engn. Trans.* **35**, 1426–1432.

Roscoe, K. H. 1970. The influence of strains in soil mechanics. *Géotechnique* **20**, 129–170.

Segall, P. & Pollard, D. D. 1980. Mechanics of discontinuous faults. *J. geophys. Res.* **85**, 4337–4350.

Sibson, R. H. 1986. Earthquakes and rock deformation in crustal fault zones. *Ann. Rev. Earth Planet. Sci.* **14**, 149–175.

Stewart, I. S. & Hancock, P. L. 1991. Scales of structural heterogeneity with neotectonic normal fault zones in the Aegean region. *J. Struct. Geol.* **13**, 191–204.

Stewart, S. A. & Bailey, H. W. 1996. The Flamborough Tertiary outlier, UK southern North Sea. *J. geol. Soc. Lond.* **153**, 163–173.

Wallace, R. E. 1986. Characteristics of faults and shear zones in deep mines. *Pure Appl. geophys.* **124**, 107–126.

Walsh, J. J. & Watterson, J. 1988. Analysis of the relationship between the displacements and dimensions of faults. *J. Struct. Geol.* **10**, 239–247.

Walsh, J. J. & Watterson, J. 1989. Displacement gradients on fault surfaces. *J. Struct. Geol.* **11**, 307–316.

Walsh, J. J. & Watterson, J. 1990. New methods of fault projection for coalmine planning. *Proc. Yorks. geol. Soc.* **48**, 209–219.

Wesnousky, S. G. 1988. Seismological and structural evolution of strike-slip faults. *Nature* **335**, 340–343.

Whitham, F. 1993. The stratigraphy of the Upper Cretaceous Flamborough Chalk Formation north of the Humber, north-east England. *Proc. Yorks. geol. Soc.* **49**, 235–258.